Evolutionary conservatism explains increasing relatedness of plant communities along a flooding gradient

Andrew J. Tanentzap[1,2,*] and William G. Lee[2,3]

[1]Ecosystems and Global Change Group, Department of Plant Sciences, University of Cambridge, Downing Street, Cambridge, CB2 3EA, United Kingdom

[2]Landcare Research, Private Bag 1930, Dunedin, New Zealand 9054

[3]School of Biological Sciences, University of Auckland, Private Bag 92019, Auckland, New Zealand

**Author for correspondence*. Telephone: +44 01223 748 982. Email: ajt65@cam.ac.uk.

Total word count for the main body of the text: 6151

Word count for Introduction: 945

Word count for Material and Methods: 2906

Word count for Results: 1199

Word count for Discussion: 993

Word count for Acknowledgements: 108

4 figures (figures 2 and 3 should be in colour), 1 table in the Main Text

4 figures, 1 table, and 2 methods supplements in Supporting Information

Brief heading: Trait conservatism increases relatedness

Summary

1. Abiotic filters have been found either to increase or reduce evolutionary relatedness in plant communities, making it difficult to generalize responses of this major feature of biodiversity to future environmental change. Here we hypothesised that the responses of phylogenetic structure to environmental change ultimately depend on how species have evolved traits for tolerating the resulting abiotic changes.
2. Working within ephemeral wetlands, we tested whether species were increasingly related as flooding duration intensified. We also identified the mechanisms underlying increased relatedness by measuring root aerenchyma volume (RAV), a trait which promotes waterlogging tolerance.
3. We found that species-specific responses to flooding explained most of the variation in occurrence for 63 vascular plant species across 5,170 plots. For a subset of 22 species, we attributed these responses to variation in RAV. Large RAV specifically increased occurrence when flooding lasted for longer time periods because large RAV reduced above-ground biomass loss. As large RAV was evolutionarily conserved within obligate wetland species, communities were more phylogenetically related as flooding increased.
4. Our study now shows how reconstructing the evolutionary history of traits that influence species' responses to environmental change can help predict future patterns in phylogenetic structure.

Key-words

disturbance, environmental filtering, functional traits, niche conservatism, phylogenetic clustering, root porosity

Introduction

Evolutionary relatedness among co-occurring species is used to understand community assembly (Webb, 2000; Kraft *et al*., 2007) and prioritize conservation actions (Isaac *et al*., 2007; Tucker *et al*., 2012), but generalizing its response to future environmental change is challenging. Many studies have reported increasing relatedness (i.e. convergence in phylogenetic structure) as environments become more stressful or disturbed (Horner-Devine & Bohannan, 2006; Cavender-Bares & Reich, 2012; Anderson *et al*., 2011; Savage & Cavender-Bares, 2012; Spasojevic & Suding, 2012; Brunbjerg *et al*., 2012; Purschke *et al*., 2013), with others finding either the reverse pattern or none at all (Bryant *et al*., 2008; Kluge & Kessler, 2011; Butterfield *et al*., 2013; Ghosh-Harihar, 2014). The general explanation for this variation – that relatedness depends on whether traits for responding to the dominant abiotic factors at a site are evolutionarily conserved – is generally assumed (Vamosi *et al*., 2009), and rarely considered as more than a statistical pattern (Cavender-Bares *et al*., 2004, 2006; Kraft *et al*., 2007; Anderson *et al*., 2011).

New process-based models now enable us to test directly how traits have evolved (Beaulieu *et al*., 2012), in order to develop clearer predictions for how phylogenetic structure and community assembly change along environmental gradients, but we are unaware of any studies that have done so. If the traits that allow species to overcome the selective forces of a given environment have not repeatedly evolved across lineages, such as because of phylogenetic restrictions over potential adaptations, then future environmental change will promote taxa that are clustered within the lineage of the regional species pool where tolerance to the new conditions evolved (Verdú & Pausas, 2007; Helmus *et al*., 2010). Such evolutionary conservatism may be the inevitable outcome of descent by modification from common ancestors (Crisp & Cook, 2012). Communities will consequently contain species that are more similar in their evolutionary history than expected by chance. By contrast, phylogenetic relatedness may be minimal if species have repeatedly converged upon similar traits with which to respond to abiotic changes. Communities will instead be comprised of species that are less closely related than expected by chance because response traits will be dispersed across lineages (Cavender-Bares *et al*., 2004). Convergent evolution may arise frequently for traits optimizing metabolic processes, such as photosynthesis (Grime, 2006), but less often for those determining responses to stress and disturbance, which can be optimized in more ways through morphology and development, as well as physiology (Donoghue & Ree, 2000).

Traits providing tolerance of a given set of abiotic conditions will certainly enable species to overcome the selective forces of a given environment, known as environmental filtering (Keddy, 1992), but the subsequent responses of phylogenetic structure will also depend on processes such as competitive exclusion and demographic stochasticity (Cavender-Bares *et al*., 2009; Mayfield & Levine, 2010). For example, close relatives can compete more intensely and exclude each other if their niches are evolutionarily conserved (Burns & Strauss, 2012), leading communities to contain species that are less related than expected by chance (Kraft *et al*., 2007). By contrast, close relatives may also have similar competitive abilities (Fritschie *et al*., 2014). If the competitive abilities of close relatives are more similar than their niches, it can lead to closely related species excluding distant relatives (Mayfield & Levine, 2010), resulting in more closely related communities (Kunstler *et al*., 2012). Opposite outcomes for phylogenetic structure can also arise in each of the two aforementioned examples where traits are convergent (Anderson *et al*., 2011). Quantifying the variation in community assembly explained by abiotic gradients relative to all other potential sources, such as species identity, can therefore help infer the importance of environmental change in driving future patterns of phylogenetic structure.

Here our aim was to provide evidence that the response of phylogenetic structure to environmental change depends upon how traits for enabling species to tolerate abiotic conditions have evolved across lineages. Our study focuses on ephemeral wetlands because these ecosystems are ideal for testing the general role of environmental change. Ephemeral wetlands have strong abiotic gradients over very short distances (i.e. metres, Tanentzap *et al*., 2013), and relatively few traits differentiating species responses (Silvertown *et al*., 1999; Mommer *et al*., 2006). We specifically focused on the evolution of a physiological trait, root aerenchyma volume (RAV), which is experimentally known to confer flooding tolerance by facilitating oxygen diffusion under waterlogging and promoting rooting depth (Justin & Armstrong, 1987; Colmer, 2003). We expected that RAV influences the fine-scale distribution of species within our community, and if so, patterns of phylogenetic structure would depend on how this trait had evolved. By combining vegetation surveys with measurements of RAV and a molecular phylogeny, we tested four sequential predictions:

(P1) More variation in site occupancy along a flooding gradient is explained by species-specific responses to flooding (i.e. interaction between species identity and flooding) than by flooding on its own or local spatial processes. Independent species sorting along environmental gradients has been long studied (Gleason, 1926; Shipley & Keddy, 1987), but here we consider its importance relative to community-level processes.

(P2) As a larger space for gas exchange can improve tolerance of hypoxia during waterlogging (Justin & Armstrong, 1987; Colmer, 2003), species that occur in sites that are flooded for longer periods will have greater maximum potential RAV.

(P3) Greater RAV is found among more closely related species than expected by chance because flooding is a strong selective force. Physiological constraints could have specifically selected against extreme values that are non-adaptive in all cases or obligate wetland species radiated adaptively around an optimum RAV, and we tried to differentiate among such potential scenarios with different macroevolutionary models.

(P4) Conservatism in RAV leads to more closely related communities as plots remain flooding for longer.

Materials and Methods

Study area

We studied six ephemeral wetlands (kettleholes) across three sites separated by between ca. 7 – 60 km in the Mackenzie Basin, South Island, New Zealand (44°11′S; 170°11′E, area: 0.68-14.9 ha). Sites developed on glacial moraines from the Late Otiran (ca. 45.0-14.5 kya), and have been relatively stable since formation (McGlone, 2009). The kettleholes are fed solely by precipitation and are typically flooded during the Austral winter and dry in summer, though water can accumulate irregularly at any time. In each kettlehole, water levels were measured every minute from December 2006 – December 2010 using Odyssey capacitance water level recorders (Dataflow Systems Ltd., Christchurch, NZ) positioned in the area of lowest elevation (see Supporting Information Fig. S1 and Methods S1). Plant communities are characterized by short prostrate plants (<3 cm tall), including herbaceous dicots and monocots, with taller shrubs sparsely positioned upslope (Table S1 in Supporting Information).

Vegetation and flooding survey

We established eight transects ranging in length from 25.4-99.7 m in each kettlehole between November 2008 and January 2009. Transects extended upslope from the central depression of each kettlehole at a random bearing within 45° intervals and at least 5 m beyond the limit of where standing water could accumulate. We randomly positioned 5 cm × 5 cm plots on average every 50 cm along each transect (range of inter-plot distances = 1 – 171 cm), and recorded the presence of all vascular species intersecting each plot (n = 5170 plots). Although superficially small, the plots are of an appropriate scale since most plants are only a

few mm in diameter, and up to 9 species can be captured within a single plot (Tanentzap *et al*., 2013). We restrict our analyses only to the 63 of 118 total species occurring in >0.2% of plots, as we could not adequately model the occurrences of species that were effectively absent from our landscape.

We estimated the flooding regime experienced within each plot by first mapping the bathymetry of each kettlehole using a laser theodolite and calculating the elevation of each plot relative to the lowest point in each kettlehole. Values ranged from 0-2.86 m, with higher elevations never flooded (Fig. S1). Relative elevations were then compared with daily mean water levels to calculate flooding duration for each plot as the number of days that each plot was submerged from Dec 2006-2011. Duration provides more information about the local flooding regime than simply the number of times each plot was flooded, but, nonetheless, is still highly correlated with other measures of flooding (Table S2).

Phylogenetic inference

We constructed a molecular-based phylogeny for our 63 study species using four markers covering both nuclear (*ITS1-5.8S-ITS2*) and plastid (*rbcL, matK, trnL-trnF*) DNA regions in order to incorporate their evolutionary relationships into our analyses (Table S1). Combining the conserved *rbcL* and *5.8S* regions with faster-evolving *matK* and noncoding *trnL* and *ITS* regions can help discriminate phylogenetic relationships within and amongst both families and genera (Kyndt *et al*., 2005). Sequences for each region were aligned using ClustalX v2.1, iterating each step to refine fit (Larkin *et al*., 2007), and we estimated tree structure and branch lengths using reversible-jump Markov chain Monte Carlo (MCMC) sampling in MrBayes v3.2 (Huelsenbeck *et al*., 2004; see Methods S1 for full details). We used a majority-rule consensus tree in our analyses, with branch lengths averaged over the trees in the posterior samples containing that branch, as all but 4 of 123 branches were present in >95% of posterior samples.

Species occurrences along flooding gradient (P1)

We tested the relative importance of species-specific responses to flooding in driving community assembly. This involved predicting the occurrence of each species in each of the 5170 plots given flooding duration, spatial scale (plot, transect and kettlehole), and species identity. Following Ives & Helmus (2011), we accounted for the fact that species can show similar mean occurrences and responses to flooding because they are phylogenetically related. We considered macroevolutionary models of both a Brownian motion, which

assumed that unobserved continuously valued traits influenced the probability of occurrence along our flooding gradient and evolved along our phylogenetic tree through random drift, and an Ornstein-Uhlenbeck (OU) process, which assumed there was selection towards a central trait value acting on the unobserved traits that influenced occurrence (see Methods S1 for full details). To test the influence of spatial processes on species occurrence among transects within each kettlehole $v_{lm}^{(1)}$, we estimated the effect of each transect from a Gaussian spatial correlation structure equal to $e^{-(\tau \mathbf{D})^2}$, where τ was the strength of the spatial correlation across all transects and **D** was a matrix of pairwise distances among the mid-points of transects in each kettlehole (Dormann *et al*., 2007). We then let the presence-absence of each species j within plot k along transect l at kettlehole site m be drawn from a Bernoulli distribution with probability p_{jklm} that was equal to:

$$\text{logit}(p_{jklm}) = \mu + v_{klm}^{(1)} + v_{lm}^{(1)} + v_{m}^{(1)} + v_{jl} + v_{jm} + v_{j}^{(1)} + v_{j}^{(2)} d_k, \quad \text{(eqn 1)}$$

where μ was the estimated mean probability of occurrence across all species that varied according to the sampled plot, transect, and kettlehole with a value of $v_{klm}^{(1)}$, $v_{lm}^{(1)}$, and $v_{m}^{(1)}$, respectively, and allowed species to differ in this response among transects and kettleholes independent of phylogenetic relatedness according to v_{jl} and v_{jm}. Including $v_{klm}^{(1)}$, $v_{lm}^{(1)}$, and $v_{m}^{(1)}$ accounted for the fact that the presences-absences of species in the same plot, among plots on the same transect, and among plots in the same kettlehole were non-independent. We also let occurrence vary among species because of phylogenetically relatedness. Relatedness changed mean occurrence according to $v_{j}^{(1)}$ and influenced the response of each species $v_{j}^{(2)}$ to flooding duration d_k. All v terms were sampled from independent zero-mean normal distributions with estimated standard deviations (SDs) to compare sources of variation in p_{jklm}.

We calculated the relative importance of both continuous effects, such as flooding duration, and factor levels, such as transect or species identity, using variance components (VCs) (Qian & Shen, 2007; Hector *et al*., 2011). Processes such as dispersal limitation and demographic stochasticity will be associated with spatial and/or residual-level variation, so we can infer the overall importance of flooding in driving community assembly by expressing its VC relative to these other factors. We estimated VCs as the SD of each v, with the SD of the residual error equal to the VC unexplained by our model (Hector *et al*., 2011).

Relating aerenchyma to occurrences along flooding gradient (P2)

We built upon our model in eqn 1 to test whether greater RAV was associated with species that occupied sites there were flooded for longer periods. This first involved measuring root aerenchyma as the proportional volume of gas space within roots (Visser & Bögemann, 2003). We focused on the 22 of the 24 most common species in our study, as these could be readily measured. For each species, we collected an average of 8 individuals (SD = 2) at regularly-spaced intervals across the flooding gradient in one of our kettleholes immediately after flooding in February 2013. In the lab, sections ca. 30 mm long were cut from root apexes of each sample and weighed before and after vacuum infiltration with water. The difference between the two weights measured the mass of the internal air space. We expressed this mass relative to the mass of infiltrated tissue multiplied by an average specific weight of infiltrated tissue (=1.036 g mL^{-1}) to derive percent root porosity. Species-specific differences in specific weight are sufficiently small that they do not measurably alter root porosities (Visser & Bögemann, 2003). For each species, we calculated maximum potential flooding tolerance RAV_{max} as the largest observed RAV. RAV_{max} therefore focused on the theoretical potential that each species could achieve. Using a population- rather than individual-level trait also eliminated the confounding effects of within-species variation on our analyses.

We then used the hierarchical modelling approach of Pollock *et al*. (2012) and Jamil *et al*. (2013) to test how the probability of occurrence of the 22 species with RAV measurements depended upon the interaction between RAV_{max} and the environment. Our approach advanced the previous methods by recognizing that species are non-independent and can show similar responses because of a shared evolutionary history. As in eqn 1, we predicted occurrence from a Bernoulli distribution with a probability p_{jklm} that depended upon flooding duration, allowing species to respond differently in each kettlehole site m:

$$\text{logit}(p_{jklm}) = \gamma_j + \beta_{j[m]}d_k + v_k^{(2)} + v_l^{(2)} + v_m^{(2)}. \quad \text{(eqn 2)}$$

The mean probability of occurrence of each species and how it was influenced RAV_{max} was given by:

$$\gamma_j = \gamma^{(1)}{}_j + \gamma^{(2)}\text{RAV}_{\text{max},j} + v_j^{(3)},$$

where $\gamma^{(1)}{}_j$ estimated species-specific mean occurrences that were not phylogenetically related, $\gamma^{(2)}$ estimated the extent to which mean occurrence changed with RAV_{max}, and $v_j^{(3)}$ reflected species-specific differences in occurrence that were phylogenetically related and estimated from pruning the larger 63 species phylogeny (Ives & Helmus, 2011). $v_j^{(3)}$ was estimated as in eqn 1 by scaling our phylogenetic tree with an estimated SD, thereby allowing phylogenetic relationships to provide additional information to RAV_{max} about the mean

occurrences of species, such as if unmeasured traits with a strong phylogenetic signal influenced species distributions (Ives & Helmus, 2011). As with eqn 1, we also tested whether transforming branch lengths in our phylogenetic tree according to an OU process was a better fit to the observed occurrence data. We tested whether RAV_{max} influenced species' responses to flooding duration in eqn 2 by expressing a species-specific slope β_j as:

$$\beta_j = \beta_1 + \beta_2 RAV_j + v_m^{(3)}. \quad (3)$$

We experimentally verified the role of RAV_{max} in conferring flood tolerance. In a previous experiment, we removed 96 16×16 cm turfs (8 cm depth) from one of the kettlehole sites and submerged them in full sun for 110, 130, 150, and 170 days (Tanentzap *et al*., 2013). Within each turf, we summed the number of times each species intersected one of 50 randomly generated coordinates at the start and immediately after each submergence period. We then calculated the maximum potential for each species to mitigate biomass loss from flooding (i.e. flooding tolerance) as the largest change in frequency observed across all pots. Here, we correlated flooding tolerance with RAV_{max} for 12 species that had both sets of trait measurements using generalised least squares that accounted for phylogenetic relatedness.

Pattern and process of aerenchyma evolution (P3)

We tested the null hypothesis that potential flooding tolerance was as different among closely related species as expected by chance. We quantified trait similarity with the *K* statistic (Blomberg *et al*., 2003), which captures the observed variance in RAV_{max} relative to that expected if it had evolved along a phylogenetic tree under a Brownian motion (BM). We compared this to a null distribution for *K* generated by randomly shuffling the tips of our phylogeny 1,000 times. We rejected our null hypothesis if the observed *K* was greater than the null distribution >95% of the time. Values greater than expected at random indicate traits are more similar among closely related species than compared with distant relatives, while values smaller than random indicate less similarity among close relatives (Blomberg *et al*., 2003). Critically, *K* alone cannot identify mechanisms generating trait distributions as similar values arise from multiple evolutionary processes, e.g. strong stabilizing selection or adaptive differentiation that slows over time (Revell *et al*., 2008).

We also sought to identify the process underlying the evolution of potential flooding tolerance across our phylogeny. We first fitted five evolutionary models to the RAV_{max} observed for each species using maximum-likelihood methods. Three models were based entirely on a BM, whereby genetic drift occurred at a rate σ_B and was either: constant (BM1); varied directionally, on average (BMD); or accelerated or decelerated exponentially over time

(ACDC), as might be expected where species radiate adaptively and variation in traits between ancestors and descendants becomes progressively smaller (Harmon *et al*., 2010). One limitation with the ACDC model is that it may be very difficult to detect without species-rich (n >50) clades at the family- or order-level and traits of extinct ancestors (Slater & Pennell, 2014). The fourth model (OU1) was based on an Ornstein–Uhlenbeck process, where species evolved towards an optimal trait value θ at a rate of α and with random noise from a BM added to this deterministic process (Hansen, 1997). The fifth model was non-evolutionary and assumed traits were normally distributed with no covariance among species (N1). Finally, we also fitted four variants that allowed evolutionary rates and optima to vary between species that were primarily restricted (i.e. obligate) versus unrestricted (i.e. facultative) to ephemeral wetlands (Methods S1). There were strong *a priori* reasons to expect selective regimes differed between obligate and facultative taxa. Specifically, obligate taxa should be pulled towards higher RAV_{max} (i.e. high θ and α; low σ_B). Facultative species may instead shift towards a smaller RAV_{max} (i.e. high α; low θ and α), because RAV has limited or no adaptive value in drier sites and/or low RAV improves the structural resistance of roots against compaction once soils dry and shrink (Striker *et al*., 2007).

All evolutionary models were estimated with the *R* packages *geiger* and *OUwie*. We compared models with the small-sampled Akaike information criterion (AICc), with smaller values indicating greater support (Burnham & Anderson, 2002). AICc was averaged among character maps for models with variable selective regimes (Methods S1). As AICc is highly sensitive to false negatives depending on the number of taxa and structure of the underlying phylogeny, we also used parametric bootstrapping to detect differences between the two best supported models (Methods S1).

Evolutionary relatedness along flooding gradient (P4)

We tested whether communities were more evolutionarily related as flooding increased. In contrast to the generalised linear mixed models described by eqns 1-2, we were interested in testing whether phylogenetic clustering at the community-level increased with flooding rather than simply identifying whether it existed. This analysis also complemented our previous models by focusing on community- rather than individual-level responses.

For each plot with >2 species (n = 2,035), we calculated the net relatedness index (NRI) as the difference between the mean phylogenetic distance (PD, i.e. branch length in the 63 species consensus tree) observed among pairs of individuals within the plot and a mean PD randomly sampled for the same number of species from across the entire phylogeny. The

null sampling therefore assumed that all 63 could hypothetically colonise all plots, which was reasonable given the spatial range of our study. The difference between observed and randomly sampled PD was then divided by the SD of the randomly sampled PD and multiplied by -1 to derive NRI. Negative and positive values denote less- and more-closely related communities than expected by chance, respectively, while values of zero are consistent with random assembly. We focused on NRI because it captures clustering from root to terminal nodes, so is more appropriate than other measures of dispersion for phylogenies driven by deep divergences with little intra-family sampling (Webb, 2000).

We tested whether NRI within each plot k along transect l at kettlehole m varied with the flooding duration experienced by that plot d_{klm} given normally-distributed error and a mean η_{klm}, which was equal to:

$$\eta_{klm} = \beta_3 + \beta_4 d_{klm} + \beta_5 \ln(s_{klm}) + v_{lm} + v_m, \quad \text{(eqn 3)}$$

where β_3 was the mean NRI across plots, β_4 was the effect of flooding, β_5 was the effect of plot-level species richness, and v_{lm} and v_m accounted for random variation among transects and kettleholes, respectively, and were each $\sim N(0, \sigma_v)$ with separately estimated σ_v's. β_5 helps control for the fact that the mean of PD can increase while its variance decreases as more species are recorded (Cadotte *et al*., 2010), potentially inflating NRI.

Model estimation and hypothesis testing (P1, P2, and P4)

We fitted all statistical models (eqns 1–3) using MCMC sampling by calling *Stan* v.2.7 from *R* (Stan Development Team, 2015). Four MCMC chains of at least 2,000 iterations were simulated for each model, with a warm-up of 1,000 runs. All regression coefficients (i.e. β's) and standard deviations (i.e. σ's) were drawn from uninformative priors that were $\sim N(0, 100)$ and $U(0, 100)$, respectively. We used a weakly informative prior for the strength of selection along our phylogeny α of $\sim N(0,1)$. All independent variables were scaled to a mean of 0 and SD of 1 prior to model estimation. Convergence was verified with standard approaches (Methods S1). *R* code to fit a *Stan* model to simulated data is given in Methods S2.

For each parameter, we calculated posterior means and 95% credible intervals (CIs) by drawing a subset of at least 1,000 simulations. We did not reject the hypothesis that the interaction between species identity and flooding was a more important driver of species occurrence than flooding on its own (P1, equation 1) if the 95% CI for the difference between the variance component of the interaction and that of flooding was ≥ 0. Similarly, we rejected null hypotheses of no effect of flooding on aerenchyma volume (P2, equation 2) and flooding on community relatedness (P4, equation 3) if 95% CIs for focal regression coefficients

excluded zero. Where we fitted different transformations of our phylogenetic tree, parameter estimates were reported only for the best supported model. Models were compared with the leave-one-out information criterion (LOOIC), which is more accurate than classical information criterion in a Bayesian context yet is interpreted similarly, i.e. smaller values indicate better supported model and we selected the more parsimonious model where differences in LOOIC were <2 (Vehtari *et al*., 2015).

Results

Species occurrences constrained by tolerance of flooding

Species-specific responses to flooding were an important driver of community assembly, supporting P1 that predicted species occurrences should change differently along a flooding gradient. For example, whilst many species were less likely to occur with increased flooding duration, there was considerable variation in prevalence and some graminoids had strong positive responses (Fig. S2). Consequently, the effect of species identity that allowed close relatives to co-vary and its interaction with flooding duration explained much more variation in the probability of occurrence of individuals than simply the mean effect of flooding (95% CIs for VCs, species × flooding interaction: 4.8 – 5.5; species identity: 4.0 – 5.0; flooding duration: 0.3 – 0.5; Fig. 1). The model allowing close relatives to co-vary without a clear directional effect was better supported than the model in which all species were concurrently drawn towards a central mean for their probability of occurrence (LOOIC for BM vs OU model: 63768 and 63816, respectively). Differences among species in occurrence across kettlehole sites and transects independent of their phylogenetic relatedness were also relatively small, suggesting that environmental responses that were not evolutionarily conserved were comparatively weak influences over community assembly (95% CIs: 2.3 – 2.9 and 1.1 – 1.3, respectively). Site-level variation in species occurrence, reflecting such factors as differences in the regional species pool, and transect- and residual-level variation, presumably associated with stochastic and spatial processes unrelated to flooding, such as dispersal limitation, were also relatively minor (for all, upper 95% CI <1.7; Fig. 1). Little variation was similarly explained at the plot-level (95% CI: 0.8 – 0.9).

We found that species occurring in sites that were flooded for longer periods had greater root aerenchyma volume as predicted by P2 (95% CI for RAV × flooding interaction effect β_2: 0.45 – 0.51). For example, a 20% increase over the observed range of flooding duration from 304 to 507 days submergence reduced the probability of occurrence of species with <20% RAV_{max} by nearly 9% (Fig. 2). By contrast, species were between 1.3 – 7.7%

more likely to occur in these conditions where RAV_{max} exceeded 30% (Fig. 2). Neither RAV_{max} or flooding duration influenced species occurrence on their own (95% CIs for $\gamma^{(2)}$ and β_1: -0.51 – 0.65 and -0.57 – 0.78, respectively), and a model of BM again better supported patterns in occurrence among close relatives (ΔLOOIC vs OU model: -4.5). Transect- and plot-level variation were also negligible in our model (for both, upper 95% CI of estimated σ <0.29) as compared with site- and species-level sources of variation in slopes and intercepts (95% CIs for σ parameters overlapping and ranging between 0.01 – 1.27). Experimental evidence suggested that high RAV_{max} minimized biomass loss during flooding (95% CI for change in frequency with logit-transformed RAV_{max}: 2.4 – 11.3), thereby favouring increased abundance by allowing individuals to exploit gaps created by the loss of species with low RAV_{max}. Species that always lost biomass during flooding (i.e. maximum change in frequency was negative) never had a RAV_{max} >25% (Fig. S3). All these results were consistent with those in the larger dataset and implicated RAV_{max} as a mechanism behind the large amount of variation explained by the species × flooding interaction in Fig. 1.

Tolerance to flooding is evolutionarily conserved

We found evidence of non-random selective forces acting upon RAV_{max}, leading to patterns of trait conservatism as predicted by P3. We specifically rejected the null hypothesis that flooding tolerance was as different among relatives as expected by chance. Close relatives were instead more similar in RAV_{max} than distant relatives (observed K = 0.59 greater than 95% of null distribution between 0.16 – 0.58).

Evolutionary models suggested that traits of ancestors were retained in descendants because of physiological constraints that stabilized onto different RAVs optimal for obligate versus facultative wetland taxa (Fig. 3). OU2 was the best supported model based on the qualitative use of AICc and variants of this model (OU2, OU2A, or OU2V) collectively accounted for almost all the support among the candidate set (Table 1). Parameter estimates were also very similar when comparing averages across the 1,000 OU2 fits versus estimates weighted across all three OU2 variants using AICc, whereby optimal RAV_{max} (logit scale) was equal to -0.84 vs -0.83, respectively, for obligate taxa, and -1.38 vs -1.56, respectively, for facultative taxa. Given these similarities, we tested whether support for the OU2 was more likely to arise than expected if trait values were derived under N1, the next best class of evolutionary models (Table 1). Reassuringly, 98.8% of the observed differences between OU2 and N1 across all 1,000 character maps were greater than the upper 95% of values expected had the underlying data been generated by N1, and we always rejected N1 when

data were simulated under OU2 (i.e. power of 100% to choose between models with false positive rate of 5%), showing that our phylogeny was sufficiently informative to detect differences in underlying trait models despite its relatively small size. Support for the OU2 model held when we compared it to the BMD, which was the next best supported non-OU model based on AICc, as differences between models were always smaller than empirical observations and we had a power of 100% to choose between these when data were simulated under a BMD. Thus, irrespective of whether OU2, OU2A, or OU2V was the best fitting model, there was strong evidence to reject a non-phylogenetic model of trait evolution.

Parameter estimates from the model with maximum likelihood across the set of 1,000 OU2 fits, each using a different ancestral character map, centred on a relatively high RAV_{max} for obligate wetland species (mean ± SE: 0.34 ± 0.03). Facultative taxa had a much lower optimum of 0.12 ± 0.04. The relatively large α (mean ± SE: 3.4 ± 1.2) and small σ_B (0.80 ± 0.53) parameters associated with this model suggested that species were rapidly drawn to their phenotypic optima (Hansen 1997), evolving half this distance in <10% of the total tree length with little confounding BM (95% confidence intervals for random change in RAV_{max} on logit-scale = -0.51 – 0.51). Model averaging with AICc across the entire set of OU2 models only strengthened these effects (α = 15.4; σ_B = 4.3; optima unchanged).

More similar communities as flooding increases

Communities were more closely related than expected by chance as flooding duration increased (Fig. 4), as predicted by P4. The net relatedness index (NRI) of plots increased with flooding duration when calculated from all the species in our phylogeny (95% CI: 0.19 – 0.28). This effect was equally strong when we calculated NRI only from the 22 taxa with RAV measurements (95% CI: 0.19 – 0.29, n = 1,491 plots), suggesting that our observations across the larger 63-species dataset were consistent with the findings that RAV_{max} determined species occurrences (Fig. 2) and was conserved across the phylogeny (Fig. 3). The increase in NRI across the 63-species dataset was also not simply due to the fact that there were fewer species in communities there were flooded for longer periods of time, and hence fewer long branch lengths, because we accounted for the variation in NRI associated with species richness in our model (95% CI: 0.03 – 0.11). A phylogenetic tree for all 63 study species is given in Supporting Information Fig. S4.

Discussion

Our findings support our central hypothesis, which predicts that environmental change should favour increasing phylogenetic relatedness where species' responses to the new conditions are evolutionarily conserved. In our study, a mean of 58% of the variation in occurrence along flooding gradients was explained by species-specific responses that allowed close relatives to vary similarly, implicating evolutionarily conservatism in species' responses (Fig. 1). By focusing on a subset of species, we then found that root aerenchyma influenced responses to flooding and was under strong selection towards habitat-specific optima (Figs 2, 3, S3). We specifically found that large RAV_{max} was conserved within obligate wetland species that tolerated flooding. This conservatism may explain why communities are more phylogenetically related as flooding increases in our study and potentially many others (e.g. Verdú & Pausas, 2007; Helmus *et al*., 2010; Ding *et al*., 2012). Patterns of phylogenetic structure may however also differ across spatial scales. For example, phylogenetic clustering may weaken within a single distributional zone, such as in plots that were never flooded, where competitive interactions can be more important controls over community assembly than environmental barriers to species establishment (Cavender-Bares *et al*., 2006).

We are also among the first to show that aerenchyma modulates species responses to changing flooding regimes in natural ecosystems. Previous studies have focused on experimentally or theoretically demonstrating the role of aerenchyma role in conferring flooding tolerance (Justin & Armstrong, 1987; Sorrell *et al*., 2000; Mommer *et al*., 2006; van Bodegom *et al*., 2008), or have shown that community-weighted mean trait values change along flood gradients (Baastrup-Spohr *et al*., 2015). Others have related the extent of aerenchyma to the maximum water depths that species occupy (e.g. Brix *et al*., 1992). Here we used the RAV of individual species to explain their specific changes in occurrence along waterlogging gradients (i.e. Fig. 2). Our results also demonstrate that measuring species responses to flooding with RAV will improve upon the subjective classification of habitat requirements widely used in the aquatic plant literature (Casanova & Brock, 2000).

Values of physiological traits enhancing plant survival are likely to be evolutionarily conserved because deviations may prove fatal where environmental filtering is strong. For example, low light availability and gas exchange are major causes of mortality during flooding (Vervuren *et al*., 2003). Here, we found support for the prediction that selection stabilised around a relatively large RAV_{max} in obligate wetland species because it promoted occupancy of flooded communities. By contrast, RAV may be non-adaptive for facultative taxa that occupy drier sites, leading to smaller values for this taxonomic group. Such strong trait-based control over environmental persistence can help explain why closely related

species retain similar levels of RAV_{max} through evolutionary time (Cooper *et al*., 2010; Crisp & Cook, 2012). Other traits for responding to environmental change may also be under strong selection towards specific trait values over evolutionary timescales (Litsios *et al*., 2014), but it remains unknown whether this process is widespread. Data syntheses suggest that stabilizing selection, for example, is not more common in plants than other forms of selection (Kingsolver & Diamond, 2011); though no explicit response traits were included in these analyses.

We cannot exclude competition as a selective force acting upon trait evolution and community assembly. Large RAV_{max} should enhance relative performance and thus resource capture because it allows plants to minimize biomass loss associated with flooding (Fig. S3). As large RAV_{max} is strongly conserved, this will create differences in competitive ability that map onto our phylogeny. Communities can therefore be more closely related than expected by chance, as observed here, because competition is the dominant force driving assembly and closely related species will be less likely to exclude each other given their similar competitive abilities (Mayfield & Levine, 2010). Such a role for competition could explain why species-specific differences unrelated to flooding influenced species occurrence (Fig. 1). However, changes in plant biomass associated with competitive interactions may be negligible relative to the effects of flooding (Lenssen *et al*., 2004), and many natural disturbances in fact change the relative competitive abilities of species (e.g. Suding & Goldberg, 2001; Fynn *et al*., 2005). Disentangling the primary driver of community assembly may thus need controlled experiments.

Our results suggest that local changes in hydrology will influence the relatedness of plant communities elsewhere if levels of RAV are strongly conserved across the tree of life. Existing data suggest that such changes in phylogenetic relatedness may be likely. Across 234 species in the Cape reeds family (Restionaceae), Huber & Linder (2012) found that aerenchyma was ancestrally present and regularly gained in wet habitats but never lost. Although we focused on considerably fewer species, null simulations showed that our phylogeny was sufficiently informative to discern similar macroevolutionary processes and our sampling across families targeted the scale at which distinct evolutionary units emerge (Barraclough & Humphreys, 2015). The presence of aerenchyma may have in fact been conserved in much of the world's flora given its ancient origins in plants that evolved ca. 300 million years ago (Green, 2010). Aerenchyma may have only been lost during the transition from waterlogged to well-drained or drier habitats (e.g. Huber & Linder, 2012), where it may pose a cost to mechanical strength of roots (Striker *et al*., 2007).

Predicting the future responses of phylogenetic structure to global change can help inform efforts to conserve uniquely evolved features, ecological functions, and the long-term capacity of biota to persist and adapt to future change (Winter *et al*., 2013). Here we have shown that reconstructing the evolution of physiological traits that influence species distributions can help provide insight into patterns of phylogenetic structure. By identifying a key trait associated with reducing biomass loss from environmental change (i.e. RAV_{max}), we predicted contemporary species occurrences, albeit on a local scale, and found that evolutionary conservatism towards high values of this trait should promote phylogenetic clustering across future communities if flooding increases. More generally, our work illustrates the value of reconstructing evolutionary history in order to predict the direction of future change in phylogenetic structure.

Acknowledgements

We thank A. Austin, S. Brockington, A. Brandt, and three anonymous reviewers for comments that improved the manuscript; G. Houliston and G. Holmes for sequencing; T. Buckley, P. Novis, R. Smissen, S. Wagstaff, and J. Beaulieu for advice with phylogenetic methods; A. Fergus for encouraging us to measure roots; and J. Comrie, P. Johnson, K. Ladley, J. Payne, G. Rogers, K. Schulz, E. Hayman, and N. Secker for help sampling. We acknowledge the use of high-performance computing facilities provided by the SCENZ-Grid cluster and New Zealand eScience Infrastructure. Funding was provided by the New Zealand Ministry of Business, Innovation and Employment in partnership with the Department of Conservation.

Author contributinos

A.J.T and W.G.L designed the research, A.J.T and W.G.L performed experiments and conducted fieldwork, A.J.T analysed data and wrote the manuscript with input from W.G.L.

References

Anderson TM, Shaw J, Olff H. **2011**. Ecology's cruel dilemma, phylogenetic trait evolution and the assembly of Serengeti plant communities. *Journal of Ecology* **99**: 797–806.

Barraclough TG, Humphreys AM. **2015**. The evolutionary reality of species and higher taxa in plants: a survey of post-modern opinion and evidence. *New Phytologist* **207**: 291–296.

Baastrup-Spohr L, Sand-Jensen K, Nicolajsen SV, Bruun HH. **2015**. From soaking wet to bone dry: predicting plant community composition along a steep hydrological gradient. *Journal of Vegetation Science* **26**, 619-630.

Beaulieu JM, Jhwueng D-C, Boettiger C, O'Meara BC. **2012**. Modeling stabilizing selection: expanding the Ornstein–Uhlenbeck model of adaptive evolution. *Evolution* **66**: 2369–2383.

Blomberg SP, Garland T, Ives AR. **2003**. Testing for phylogenetic signal in comparative data: behavioral traits are more labile. *Evolution* **57**: 717–745.

Brix H, Orr PT. **1992**. Internal pressurization and convective gas flow in some emergent freshwater macrophytes. *Limnology and Oceanography* **37**: 1420–1433.

Brunbjerg AK, Borchsenius F, Eiserhardt WL, Ejrnæs R, Svenning J-C. **2012**. Disturbance drives phylogenetic community structure in coastal dune vegetation. *Journal of Vegetation Science* **23**: 1082–1094.

Bryant JA, Lamanna C, Morlon H, Kerkhoff AJ, Enquist BJ, Green JL. **2008**. Microbes on mountainsides: Contrasting elevational patterns of bacterial and plant diversity. *Proceedings of the National Academy of Sciences of the United States of America* **105**: 11505–11511.

Burnham KP, Anderson DR. 2002. *Model selection and multimodel inference: a practical information-theoretic approach*. New York, USA: Springer-Verlag.

Burns JH, Strauss SY. **2011**. More closely related species are more ecologically similar in an experimental test. *Proceedings of the National Academy of Sciences* **108**: 5302–5307.

Butterfield BJ, Cavieres LA, Callaway RM, Cook BJ, Kikvidze Z, Lortie CJ, Michalet R, Pugnaire FI, Schöb C, Xiao S, *et al.* 2013. Alpine cushion plants inhibit the loss of phylogenetic diversity in severe environments. *Ecology Letters* **16**: 478–486.

Cadotte MW, Borer ET, Seabloom EW, Cavender-Bares J, Harpole WS, Cleland E, Davies KF. **2010**. Phylogenetic patterns differ for native and exotic plant communities across a richness gradient in Northern California. *Diversity and Distributions* **16**: 892–901.

Casanova MT, Brock MA. **2000**. How do depth, duration and frequency of flooding influence the establishment of wetland plant communities? *Plant Ecology* **147**: 237–250.

Cavender-Bares J, Ackerly DD, Baum DA, Bazzaz FA. **2004**. Phylogenetic overdispersion in Floridian oak communities. *American Naturalist* **163**: 823–843.

Cavender-Bares J, Keen A, Miles B. **2006**. Phylogenetic structure of Floridian plant communities depends on taxonomic and spatial scale. *Ecology* **87**: S109–S122.

583 **Cavender-Bares J, Kozak KH, Fine PVA, Kembel SW**. **2009**. The merging of community
584 ecology and phylogenetic biology. *Ecology Letters* **12**: 693–715.
585 **Cavender-Bares J, Reich PB**. **2012**. Shocks to the system: community assembly of the oak
586 savanna in a 40-year fire frequency experiment. *Ecology* **93**: S52–S69.
587 **Colmer TD**. **2003**. Long-distance transport of gases in plants: a perspective on internal
588 aeration and radial oxygen loss from roots. *Plant Cell and Environment* **26**, 17-36.
589 **Cooper N, Jetz W, Freckleton RP**. **2010**. Phylogenetic comparative approaches for studying
590 niche conservatism. *Journal of Evolutionary Biology* **23**: 2529–2539.
591 **Crisp MD, Cook LG**. **2012**. Phylogenetic niche conservatism: what are the underlying
592 evolutionary and ecological causes? *New Phytologist* **196**: 681–694.
593 **Deil U**. **2005**. A review on habitats, plant traits and vegetation of ephemeral wetlands – a
594 global perspective. *Phytocoenologia* **35**: 533–706.
595 **Ding Y, Zang R, Letcher SG, Liu S, He F**. **2012**. Disturbance regime changes the trait
596 distribution, phylogenetic structure and community assembly of tropical rain forests.
597 *Oikos* **121**: 1263–1270.
598 **Donoghue MJ, Ree RH**. **2000**. Homoplasy and developmental constraint: a model and an
599 example from plants. *American Zoologist* **40**: 759–769.
600 **Dormann RC, McPherson MJ, Araújo BM, Bivand R, Bolliger J, Carl G, Davies GR,**
601 **Hirzel A, Jetz W, Kissling DW, *et al.* 2007**. Methods to account for spatial
602 autocorrelation in the analysis of species distributional data: a review. *Ecography* **30**: 609–
603 628.
604 **Fritschie KJ, Cardinale BJ, Alexandrou MA, Oakley TH**. **2014**. Evolutionary history and
605 the strength of species interactions: testing the phylogenetic limiting similarity hypothesis.
606 *Ecology* **95**: 1407–1417.
607 **Fynn RWS, Morris CD, Kirkman KP. 2005**. Plant strategies and trait trade-offs influence
608 trends in competitive ability along gradients of soil fertility and disturbance. *Journal of*
609 *Ecology* **93**: 384–394.
610 **Ghosh-Harihar M**. **2014**. Phylogenetic and ecomorphological structure of assemblages of
611 breeding leaf warblers (Phylloscopidae) along Himalayan elevational gradients. *Journal of*
612 *Biogeography* **41**: 1193–1203.
613 **Gleason HA**. **1926**. The individualistic concept of the plant association. *Bulletin of the*
614 *Torrey Botanical Club* **53**: 7–26.
615 **Green WA**. **2010**. The function of the aerenchyma in arborescent lycopsids: evidence of an
616 unfamiliar metabolic strategy. *Proceedings of the Royal Society B* **277**: 2257–2267.

Grime JP. **2006**. Trait convergence and trait divergence in herbaceous plant communities: Mechanisms and consequences. *Journal of Vegetation Science* **17**: 255–260.

Hansen TF. **1997**. Stabilizing selection and the comparative analysis of adaptation. *Evolution* **51**: 1341–1351.

Harmon LJ, Losos JB, Jonathan Davies T, Gillespie RG, Gittleman JL, Bryan Jennings W, Kozak KH, McPeek MA, Moreno-Roark F, Near TJ, *et al.* 2010. Early bursts of body size and shape evolution are rare in comparative data. *Evolution* **64**: 2385–2396.

Hector A, Bell T, Hautier Y, Isbell F, Kéry M, Reich PB, Ruijven J van, Schmid B. **2011**. BUGS in the analysis of biodiversity experiments: species richness and composition are of similar importance for grassland productivity. *PLoS ONE* **6**: e17434.

Helmus MR, Keller W (Bill), Paterson MJ, Yan ND, Cannon CH, Rusak JA. **2010**. Communities contain closely related species during ecosystem disturbance. *Ecology Letters* **13**: 162–174.

Horner-Devine MC, Bohannan BJM. **2006**. Phylogenetic clustering and overdispersion in bacterial communities. *Ecology* **87**: S100–S108.

Huber M, Linder HP. **2012**. The evolutionary loss of aerenchyma limits both realized and fundamental ecohydrological niches in the Cape reeds (Restionaceae). *Journal of Ecology* **100**: 1338–1348.

Huelsenbeck JP, Larget B, Alfaro ME. **2004**. Bayesian phylogenetic model selection using reversible jump Markov chain Monte Carlo. *Molecular Biology and Evolution* **21**: 1123–1133.

Isaac NJB, Turvey ST, Collen B, Waterman C, Baillie JEM. **2007**. Mammals on the EDGE: Conservation Priorities Based on Threat and Phylogeny. *PLoS ONE* **2**: e296.

Ives AR, Helmus MR. **2011**. Generalized linear mixed models for phylogenetic analyses of community structure. *Ecological Monographs* **81**: 511–525.

Jamil T, Ozinga WA, Kleyer M, ter Braak CJF. **2013**. Selecting traits that explain species–environment relationships: a generalized linear mixed model approach. *Journal of Vegetation Science* **24**: 988–1000.

Johnson P, Rogers G. 2003. Ephemeral wetlands and their turfs in New Zealand. *Science for Conservation* **230**: 1–109.

Justin SHFW, Armstrong W. **1987**. The anatomical characteristics of roots and plant response to soil flooding. *New Phytologist* **106**: 465–495.

Keddy PA. **1992**. Assembly and response rules: two goals for predictive community ecology. *Journal of Vegetation Science* **3**: 157–164.

Kingsolver JG, Diamond SE. **2011**. Phenotypic selection in natural populations: what limits directional selection? *American Naturalist* **177**: 346–357.

Kluge J, Kessler M. **2011**. Phylogenetic diversity, trait diversity and niches: species assembly of ferns along a tropical elevational gradient. *Journal of Biogeography* **38**: 394–405.

Kraft NJB, Cornwell WK, Webb CO, Ackerly DD. **2007**. Trait evolution, community assembly, and the phylogenetic structure of ecological communities. *American Naturalist* **170**: 271–283.

Kunstler G, Lavergne S, Courbaud B, Thuiller W, Vieilledent G, Zimmermann NE, Kattge J, Coomes DA. **2012**. Competitive interactions between forest trees are driven by species' trait hierarchy, not phylogenetic or functional similarity: implications for forest community assembly. *Ecology Letters* **15**: 831–840.

Kyndt T, Van Droogenbroeck B, Romeijn-Peeters E, Romero-Motochi JP, Scheldeman X, Goetghebeur P, Van Damme P, Gheysen G. **2005**. Molecular phylogeny and evolution of Caricaceae based on rDNA internal transcribed spacers and chloroplast sequence data. *Molecular Phylogenetics and Evolution* **37**: 442–459.

Larkin MA, Blackshields G, Brown NP, Chenna R, McGettigan PA, McWilliam H, Valentin F, Wallace IM, Wilm A, Lopez R, *et al.* 2007. Clustal W and Clustal X version 2.0. *Bioinformatics* **23**: 2947–2948.

Lenssen JPM, van de Steeg HM, de Kroon H. **2004**. Does disturbance favour weak competitors? Mechanisms of changing plant abundance after flooding. *Journal of Vegetation Science* **15**: 305–314.

Litsios G, Wüest RO, Kostikova A, Forest F, Lexer C, Linder HP, Pearman PB, Zimmermann NE, Salamin N. **2014**. Effects of a fire response trait on diversification in replicated radiations. *Evolution* **68**: 453–465.

Mayfield MM, Levine JM. **2010**. Opposing effects of competitive exclusion on the phylogenetic structure of communities. *Ecology Letters* **13**: 1085–1093.

McGlone MS. **2009**. Postglacial history of New Zealand wetlands and implications for their conservation. *New Zealand Journal of Ecology* **33**: 1–23.

Mommer L, Lenssen JPM, Huber H, Visser EJW, De Kroon H. **2006**. Ecophysiological determinants of plant performance under flooding: a comparative study of seven plant families. *Journal of Ecology* **94**: 1117–1129.

Pollock LJ, Morris WK, Vesk PA. **2012**. The role of functional traits in species distributions revealed through a hierarchical model. *Ecography* **35**: 716–725.

Purschke O, Schmid BC, Sykes MT, Poschlod P, Michalski SG, Durka W, Kühn I, Winter M, Prentice HC. **2013**. Contrasting changes in taxonomic, phylogenetic and functional diversity during a long-term succession: insights into assembly processes. *Journal of Ecology* **101**: 857–866.

Qian SS, Shen Z. **2007**. Ecological applications of multilevel analysis of variance. *Ecology* **88**: 2489–2495.

Revell LJ, Harmon LJ, Collar DC. **2008**. Phylogenetic signal, evolutionary process, and rate. *Systematic Biology* **57**: 591–601.

Savage JA, Cavender-Bares J. **2012**. Habitat specialization and the role of trait lability in structuring diverse willow (genus *Salix*) communities. *Ecology* **93**: S138–S150.

Shipley B, Keddy PA. **1987**. The individualistic and community-unit concepts as falsifiable hypotheses. *Vegetatio* **69**: 47–55.

Silvertown J, Dodd ME, Gowing DJG, Mountford JO. **1999**. Hydrologically defined niches reveal a basis for species richness in plant communities. *Nature* **400**: 61–63.

Slater GJ, Pennell MW. **2014**. Robust regression and posterior predictive simulation increase power to detect early bursts of trait evolution. *Systematic Biology* **63**: 293–308.

Sorrell BK, Mendelssoh IA, Mckee KL, Woods RA. **2000**. Ecophysiology of wetland plant roots: a modelling comparison of aeration in relation to species distribution. *Annals of Botany* **86**: 675–685.

Spasojevic MJ, Suding KN. **2012**. Inferring community assembly mechanisms from functional diversity patterns: the importance of multiple assembly processes. *Journal of Ecology* **100**: 652–661.

Stan Development Team. 2015. *Stan: A C++ Library for probability and sampling, version 2.7*. [WWW document] URL http://mc-stan.org/. [accessed 26 May 2016].

Stephens PR, Wiens JJ. **2004**. Convergence, divergence, and homogenization in the ecological structure of emydid turtle communities: the effects of phylogeny and dispersal. *American Naturalist* **164**: 244–254.

Striker GG, Insausti P, Grimoldi AA, Vega AS. **2007**. Trade-off between root porosity and mechanical strength in species with different types of aerenchyma. *Plant, Cell & Environment* **30**: 580–589.

Suding KN, Goldberg D. **2001**. Do disturbances alter competitive hierarchies? Mechanisms of change following gap creation. *Ecology* **82**: 2133–2149.

Tanentzap AJ, Lee WG, Schulz KAC. **2013**. Niches drive peaked and positive relationships between diversity and disturbance in natural ecosystems. *Ecosphere* **4**: art133.

Tucker CM, Cadotte MW, Davies TJ, Rebelo TG. **2012**. Incorporating geographical and evolutionary rarity into conservation prioritization. *Conservation Biology* **26**: 593–601.

Vamosi SM, Heard SB, Vamosi JC, Webb CO. **2009**. Emerging patterns in the comparative analysis of phylogenetic community structure. *Molecular Ecology* **18**: 572–592.

van Bodegom PM, Sorrell BK, Oosthoek A, Bakker C, Aerts R. **2008**. Separating the effects of partial submergence and soil oxygen demand on plant physiology. *Ecology* **89**: 193–204.

Vehtari A, Gelman A, Gabry J. **2015**. Practical Bayesian model evaluation using leave-one-out cross-validation and WAIC. *arXiv:1507.04544 [stat]*.

Verdú M, Pausas JG. **2007**. Fire drives phylogenetic clustering in Mediterranean Basin woody plant communities. *Journal of Ecology* **95**: 1316–1323.

Vervuren PJA, Blom CWPM, De Kroon H. **2003**. Extreme flooding events on the Rhine and the survival and distribution of riparian plant species. *Journal of Ecology* **91**: 135–146.

Visser EJW, Bögemann GM. **2003**. Measurement of porosity in very small samples of plant tissue. *Plant and Soil* **253**: 81–90.

Webb CO, Losos AEJB. **2000**. Exploring the phylogenetic structure of ecological communities: an example for rain forest trees. *American Naturalist* **156**: 145–155.

Winter M, Devictor V, Schweiger O. **2013**. Phylogenetic diversity and nature conservation: where are we? *Trends in Ecology & Evolution* **28**: 199–204.

Supporting Information

Additional supporting information may be found in the online version of this article:

Fig. S1 Temporal trends in flooding.

Fig. S2 Species occurrence along flooding gradient.

Fig. S3 Biomass loss during submergence versus root aerenchyma volume.

Fig. S4 Phylogenetic hypothesis for 63 wetland species.

Table S1 Genetic markers for study species.

Table S2 Correlations among measures of flooding regime.

Methods S1 Additional methods.

Methods S2 Stan code for fitting a model with phylogenetic effects.

Please note: Wiley-Blackwell are not responsible for the content or functionality of any supporting information supplied by the authors. Any queries (other than missing material) should be directed to the New Phytologist Central Office.

Table 1. Evolutionary models fitted to maximum root aerenchyma volume (RAV_{max}) observed for 22 species. Models were based on either: a Brownian motion with drift that was constant (BM1), varied directionally (BMD), accelerated or decelerated exponentially over time (ACDC), or constant at different rates between obligate and facultative wetland species (BM2); an Ornstein–Uhlenbeck process with the same optimal trait value (θ), rate of attraction towards the trait optima (α), and random noise (σ) across all species (OU1), or a different θ (OU2), both θ and α (OU2A), or both θ and σ (OU2V) between obligate and facultative wetland species; or a non-evolutionary process that assumed no covariance among species (N1). Best supported model bolded. AICc weight (w_i) is proportion of support for a model out of given candidate set. *Averaged across 1,000 model fits, each with a different character map.

model	AICc	w_i
OU2*	**30.8**	**0.66**
OU2A*	33.5	0.17
OU2V*	33.9	0.14
N1	38.5	0.01
OU1	40.4	0.01
BMD*	41.8	<0.01
BM1	42.3	<0.01
ACDC	42.7	<0.01
BM2	43.8	<0.01

Figure Legends

Fig. 1. Mean ± 95% CIs for variance components (standard deviation scale) explaining probability of occurrence of 63 species across 5,170 vegetation plots. Overall, the model correctly classified most observations, as measured by a large proportion of explained cross-validated deviance (= 0.51) and an area under a receiver operating characteristic curve (AUC) of 0.97, which represents the probability that a species presence will be scored higher than an absence. Spp_{phylo} and $Spp_{non\text{-}phylo}$ respectively represent species-specific responses that either were or were not phylogenetically-related and these effects were only moderately inter-correlated (absolute Spearman's ρ for all pair-wise comparisons among variance components <0.50).

Fig. 2. Large root porosity increases probability of occurrence as flooding duration lasts longer. We plotted the change in the percent probability of occurrence in 22 species from a 20% increase in flooding duration versus their maximum potential root aerenchyma volume, measured as porosity. Solid line is mean model fit and shaded area is 95% CI. Proportion of cross-validated deviance explained and AUC for the overall model were 0.81 and 0.81, respectively.

Fig 3. Phylogram for 22 wetland species with measurements of maximum root aerenchyma volume (RAV_{max}) scaled with symbol size from 10–40%. The phylogram was generated by dropping tips lacking trait data from a Bayesian majority-rule consensus tree estimated for all our 63 study species (Fig. S4). Branch colours are posterior probability (PP) of habitat affinity being either obligate (O, green) or facultative (F, blue) to wetlands.

Fig. 4. Communities are increasingly related as flooding duration increases. For plotting only, points were averages ± standard error of ca. 250 plot-level observations at the median of each of 8 duration-class bins. Solid line is mean change in net relatedness index (NRI) with flooding duration at mean values of all other predictor variables in eqn 3. Shaded area denotes 95% CI. Lines adjacent to axes denote the positions of flooding duration and NRI within the plotted range.

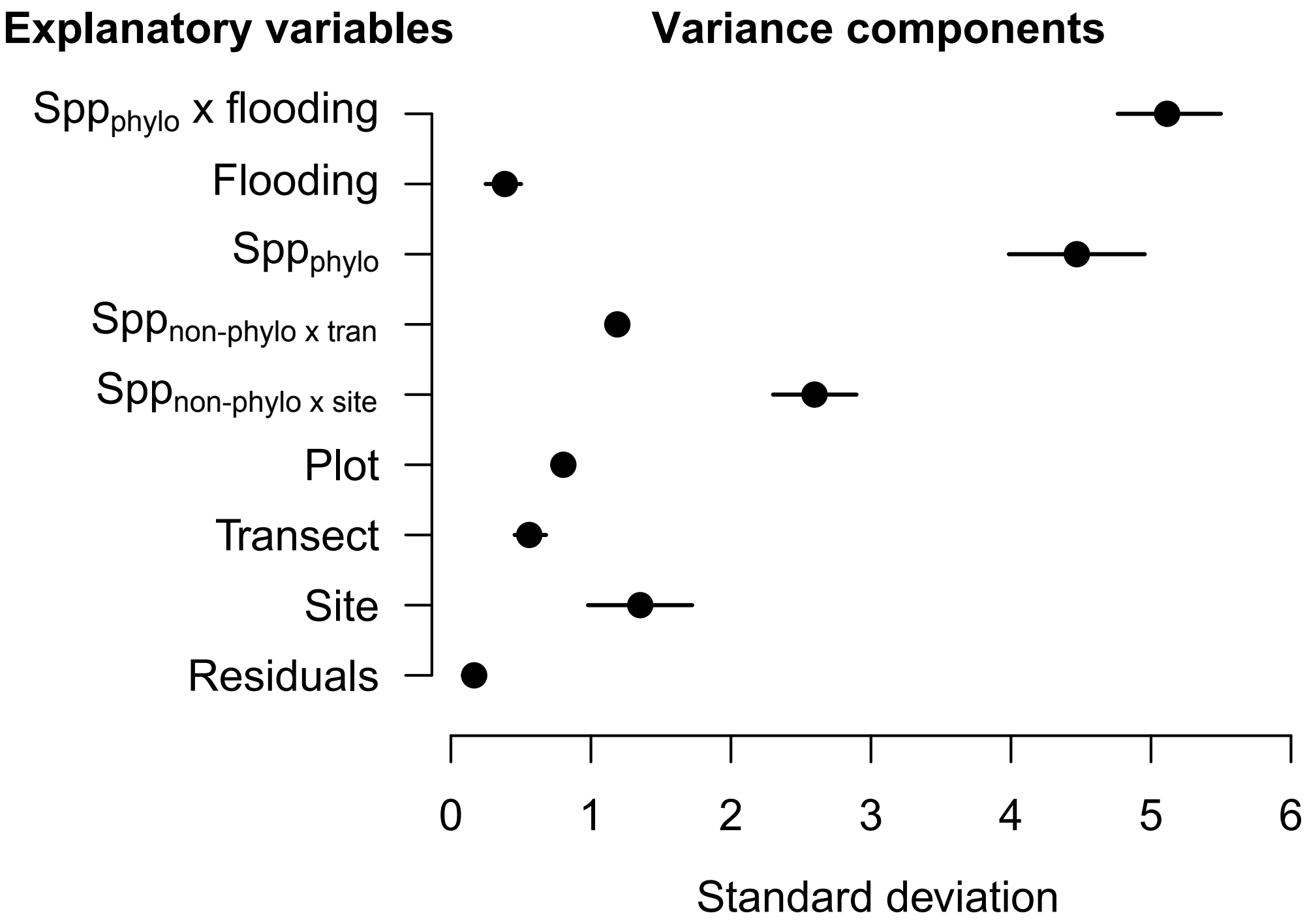
Explanatory variables
Variance components
Spp phylo x flooding
Flooding
Spp phylo
Spp non-phylo x tran
Spp non-phylo x site
Plot
Transect
Site
Residuals
0
1
2
3
4
5
6
Standard deviation

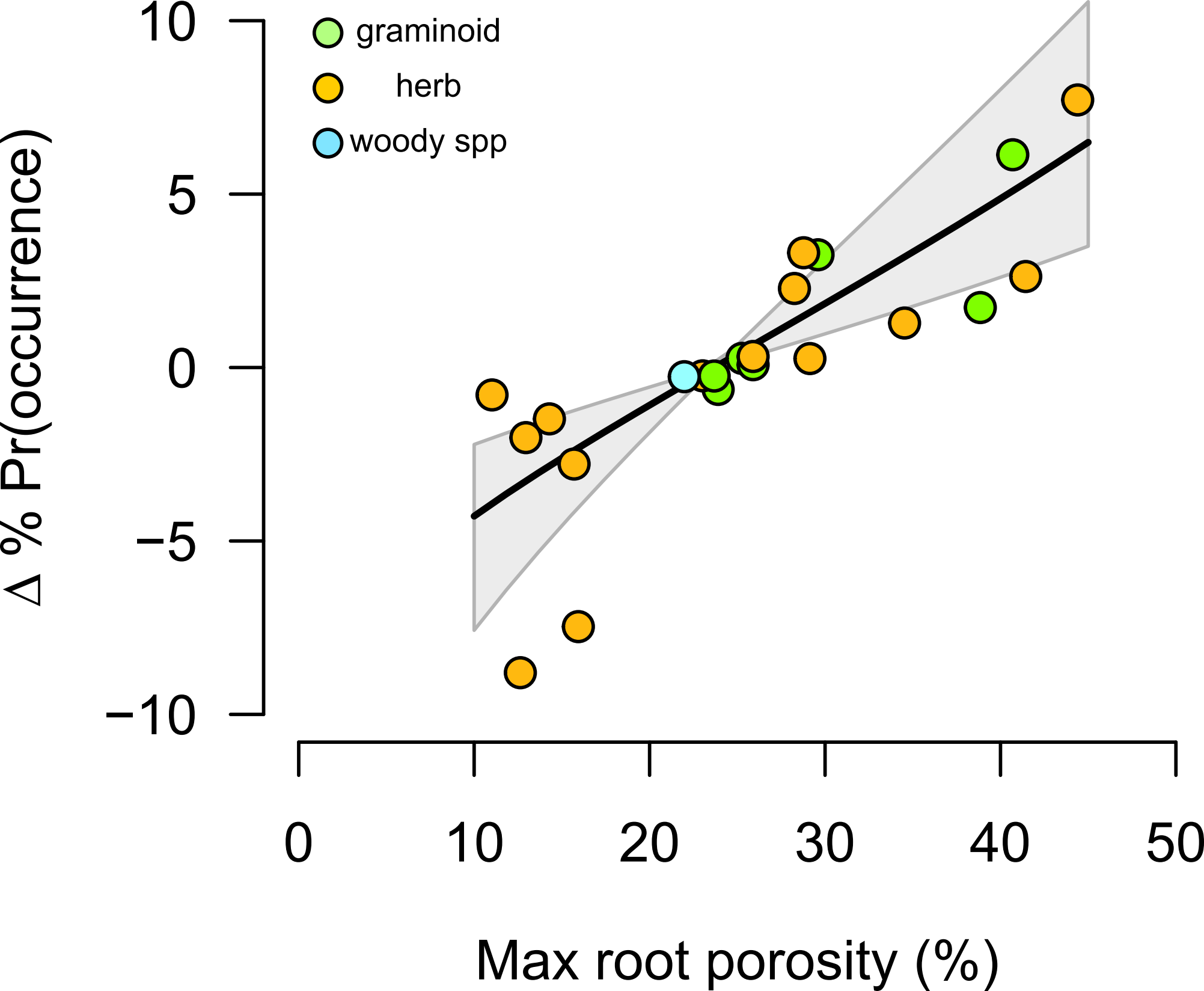
graminoid
herb
woody spp
10
5
0
−5
−10
Δ % Pr(occurrence)
0
10
20
30
40
50
Max root porosity (%)

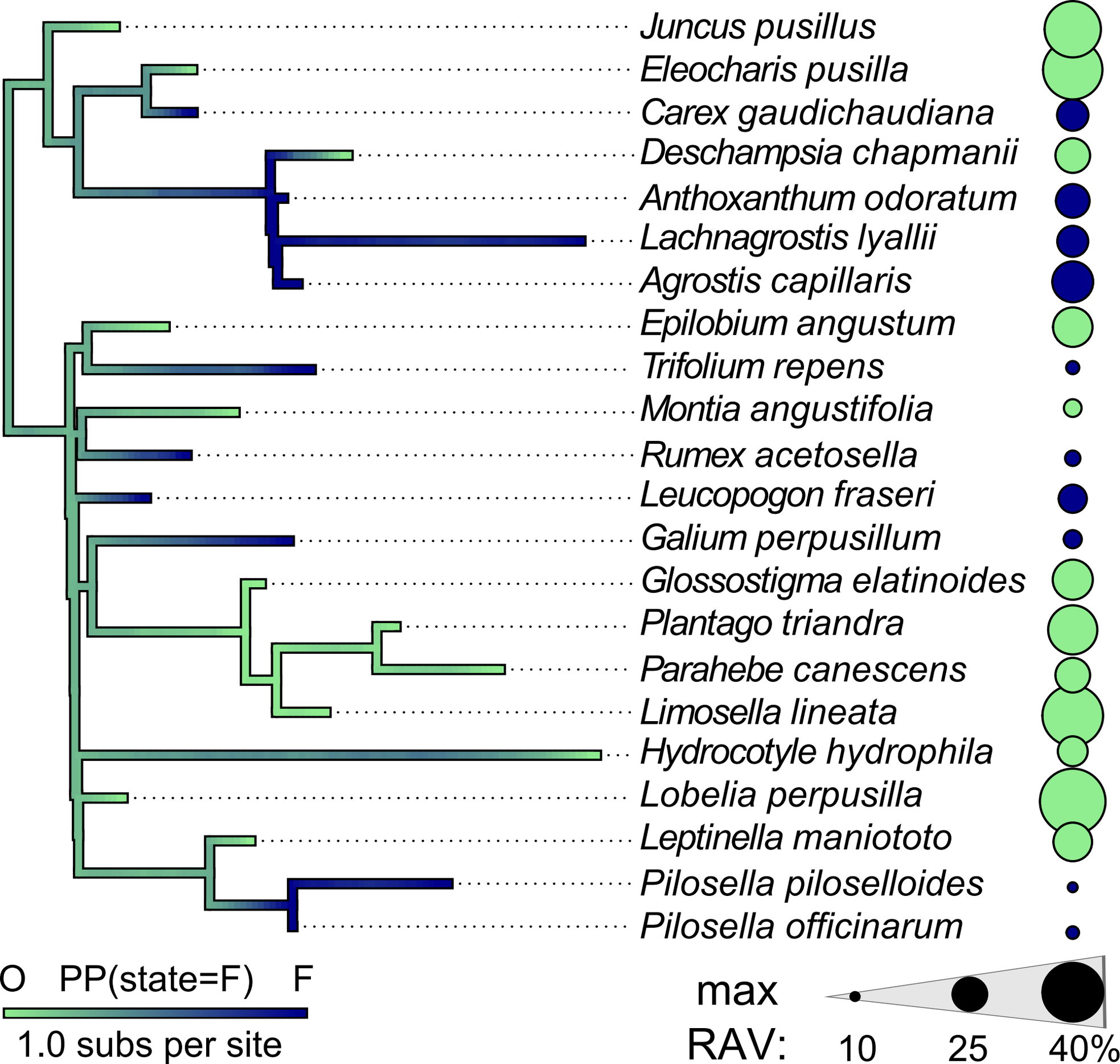
Juncus pusillus
Eleocharis pusilla
Carex gaudichaudiana
Deschampsia chapmanii
Anthoxanthum odoratum
Lachnagrostis lyallii
Agrostis capillaris
Epilobium angustum
Trifolium repens
Montia angustifolia
Rumex acetosella
Leucopogon fraseri
Galium perpusillum
Glossostigma elatinoides
Plantago triandra
Parahebe canescens
Limosella lineata
Hydrocotyle hydrophila
Lobelia perpusilla
Leptinella maniototo
Pilosella piloselloides
Pilosella officinarum
O PP(state=F) F
1.0 subs per site
max
RAV:
10
25
40%

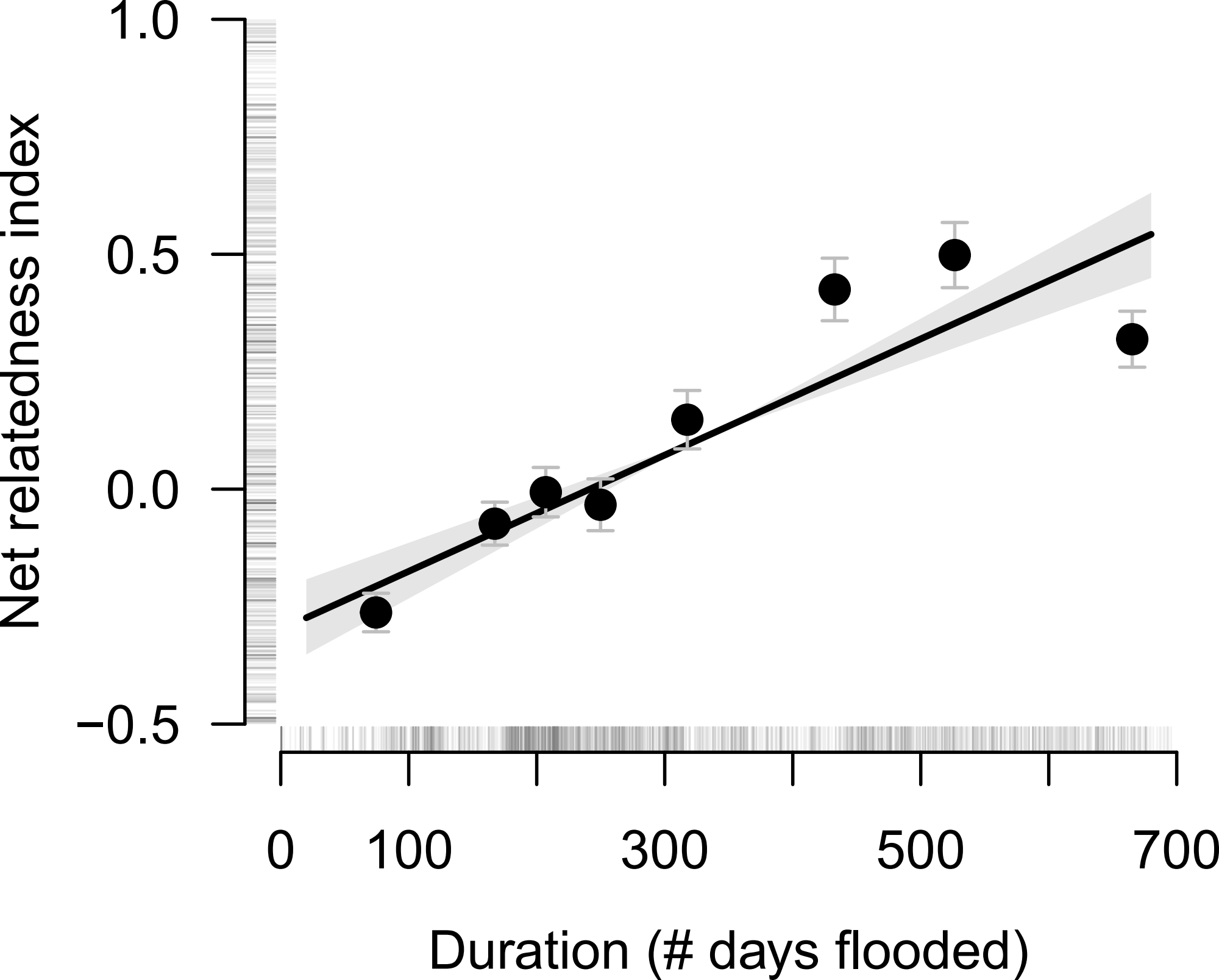
1.0
0.5
0.0
−0.5
Net relatedness index
0
100
300
500
700
Duration (# days flooded)